4. V. T. Chemeris and A. D. Podol'tsev, "Computer investigation of the magnetopulse interaction of conducting circuits taking into account the motion of the secondary circuit," Tekh. Elektrodin., No. 1 (1979).
5. P. L. Kalantarov and L. A. Tseitlin, Inductance Calculations [in Russian], Énergiya, Leningrad (1970).
6. K. Hartman, E. Letskii, and V. Shafer, Planning of an Experiment in Research and Technological Processes [Russian translation], Mir, Moscow (1977).

NUMERICAL INVESTIGATION OF THE PROCESSES IN A PLASMATRON WITH KEEN BLOWING

V. I. Artemov and O. A. Sinkevich

UDC 539.95

High-enthalpy plasmatrons are an important element of new industrial technology at the present time because of the possibility of obtaining rapid heating of a wide range of gases (including chemically active gases such as hydrogen, oxygen, chlorine etc.) up to high temperatures ($2\text{-}3\cdot10^4$°K) at working pressures of up to 10^7 Pa. One of the main problems in constructing such plasmatrons is to increase the specific energy contribution to the electric arc. Since the current flowing through the plasmatron has an upper limit set by the permissible erosion of the electrodes, to increase the power it is necessary to increase the electric field in the arc. One can obtain effective control of the electric field by blowing gas either in the intersection slots or through a porous interelectrode mounting [1]. One form of blowing is keen blowing, when gas is blown through one of the intersection slots with a flow rate of the order of or greater than the main flow. In this case the electric field in the arc and the temperature are increased, a gas curtain is formed on the walls of the plasmatron which enables the temperature of the wall to be maintained within the desired limits, and the boundary layer breaks up, leading to a hydrodynamically developed flow. Experimental investigations [1, 2] have been devoted mainly to analyzing the integral parameters: the current–voltage characteristics, the thermal efficiency, the mean-mass enthalpy, etc. This is mainly due to the difficulties involved in making measurements of the local characteristics, although when designing plasmatrons the latter play an important role.

To calculate the local parameters, numerical methods of analysis are promising, but even their use involves a number of difficulties. The complex structure of the flow of gas, and the impossibility of distinguishing the characteristic direction of motion make numerical calculations based on the boundary-layer approximation, which is mainly employed to investigate arcs in the plasmatron [3, 4], very inefficient. For a flow rate of the gas in the blowing through the walls of the order of the main flow rate, finite-difference algorithms cease to converge. Numerical simulation of the arc using the solution of the complete Navier–Stokes equations is the most acceptable. Using this method, investigations have been made [5] of the electric arc in the initial part of the plasmatron [6, 7] and in the case when there is intense blowing of gas through a porous wall [8]. These papers domonstrate the possibility of using numerical methods developed mainly for an incompressible liquid, and there is good qualitative agreement with experiments. In the present paper, using the complete Navier–Stokes equations we investigate the electric arc in a sectioned channel of a plasmatron with intense local gas blowing; the arc parameters are chosen to be such that a comparison can be made with experimental data [2] in order to estimate the efficiency of the method.

1. To describe the flow of an equilibrium plasma in the channel we will use the complete system of Navier–Stokes equations taking into account radiation transfer and Joule heat dissipation. By changing to the vortex-current function variable and using the assumptions employed in [3, 9], usually used when investigating an arc, the system of equations in the axisymmetrical stationary case can be reduced to the form [5]

$$r^2\left[\frac{\partial}{\partial z}\left(\frac{\Omega}{r}\frac{\partial\Phi}{\partial r}\right)-\frac{\partial}{\partial r}\left(\frac{\Omega}{r}\frac{\partial\Phi}{\partial z}\right)\right]-\frac{\partial}{\partial z}\left[r^3\frac{\partial}{dz}\left(\mu\frac{\Omega}{r}\right)\right]- \qquad (1.1)$$

Moscow. Translated from Zhurnal Prikladnoi Mekhaniki i Tekhnicheskoi Fiziki, No. 2, pp. 87-91, March-April, 1983. Original article submitted January 26, 1982.

0021-8944/83/2402-0215$07.50

$$-\frac{\partial}{\partial r}\left[r^3\frac{\partial}{\partial r}\left(\mu\frac{\Omega}{r}\right)\right]=r^2\left[\frac{\partial}{\partial z}\left(\frac{u_z^2+u_r^2}{2}\right)\frac{\partial\rho}{\partial r}-\frac{\partial}{\partial r}\left(\frac{u_z^2+u_r^2}{2}\right)\frac{\partial\rho}{\partial z}-rS_\Omega-\frac{\mu_e}{r^3}\frac{\partial\Psi^2}{\partial z}\right],$$

$$\frac{\partial}{\partial z}\left(\frac{1}{\rho r}\frac{\partial\Phi}{\partial z}\right)+\frac{\partial}{\partial r}\left(\frac{1}{\rho r}\frac{\partial\Phi}{\partial r}\right)=-\Omega,$$

$$\frac{\partial}{\partial z}\left(H\frac{\partial\Phi}{\partial r}\right)-\frac{\partial}{\partial r}\left(H\frac{\partial\Phi}{\partial z}\right)-\frac{\partial}{\partial z}\left(r\frac{\lambda}{c_p}\frac{\partial H}{\partial z}\right)-\frac{\partial}{\partial r}\left(r\frac{\lambda}{c_p}\frac{\partial H}{\partial r}\right)=\frac{1}{\sigma r}\left[\left(\frac{\partial\Psi}{\partial z}\right)^2+\left(\frac{\partial\Psi}{\partial r}\right)^2\right]-rF_R,$$

$$\frac{\partial}{\partial z}\left(\frac{1}{\sigma r}\frac{\partial\Psi}{\partial z}\right)+\frac{\partial}{\partial r}\left(\frac{1}{\sigma r}\frac{\partial\Psi}{\partial r}\right)=0,$$

where Ω is the vortex intensity ($\Omega = \partial u_r/\partial z - \partial u_z/\partial r$), Φ is the current function, connected with the components of the velocity vector (u_z, u_r) by the relations

$$u_z=\frac{1}{\rho r}\frac{\partial\Phi}{\partial r},\quad u_r=-\frac{1}{\rho r}\frac{\partial\Phi}{\partial z};$$

H is the enthalpy, Ψ is the electric-current function

$$E_z=\frac{1}{\sigma r}\frac{\partial\Psi}{\partial r},\quad E_r=-\frac{1}{\sigma r}\frac{\partial\Psi}{\partial z};\tag{1.2}$$

ρ, c_p, μ, λ, σ are the density, heat capacity at constant pressure, the viscosity, the thermal conductivity, and the electrical conductivity, respectively, and F_R takes into account the losses due to radiation in the optically transparent part of the spectrum. The pressure distribution can be found by simple integration, and to calculate the derivatives $\partial p/\partial z$ and $\partial p/\partial r$ one can use the initial Navier–Stokes equations. The function S_Ω includes the second derivatives of the viscosity with respect to the coordinates, and its form is given in [5].

The boundary conditions for the vortex intensity on the electrodes and on the walls can be found from the adhesion conditions. We used both the condition of first order of accuracy, and the boundary condition of the second order [10], and in the latter case, to stabilize the instability which occurs, we employed an "implicit scheme" for calculating the vortex intensity at the boundary points [5]. At the input the vortex intensity was found by differentiating the specified velocity profile, and on the axis of symmetry we assumed that the following holds:

$$\Omega = ar + br^2,\quad r\to 0.$$

The current function Φ on the electrodes, the walls, and the axis of symmetry is constant, and at the input it was found by integrating the velocity profile. The enthalpy on the walls, the input, and the electrode is constant and equal to H_i, H_w, and H_e, respectively. The specification of constant enthalpy on the electrode strictly speaking does not correspond to the truth, but this condition is no worse than specifying the enthalpy profile obtained by solving the Elenbaas–Heller equation for a channel of radius r_K, as was done in [6-8], since the calculations carried out there demonstrated that H_e has only a slight effect on the solution, with the exception of a narrow region close to the electrode. At the input, on the walls, and on the axis of symmetry the electric-current function Ψ is constant, and on the electrodes we used the condition for there to be no electric field along an ideally conducting electrode $\partial\Psi/\partial n = 0$, where n is the vector normal to the electrode. At the output of the channel, as in [5], we assumed that $\partial\Omega/\partial z = \partial\Phi/\partial z = \partial H/\partial z = \partial\Psi/\partial z = 0$.

The finite-difference analog of system (1.1) was solved by the Gauss–Seidel method using the algorithm proposed in [5], in a rectangular region in the (z, r) plane (Fig. 1). To extend the region of convergence with respect to the Reynolds number, we used the approximation of the convective terms to a first order of accuracy (the "opposite flow" difference [5]). The considerable nonlinearity of system (1.1) due to the dependence of the transfer coefficients on the enthalpy may also be the reason for the divergence of the iterational process. In this case we used the following methods to obtain stable convergence: 1) the method of lower relaxation, not only for the basic variables Ω, Φ, H, Ψ but also for the source terms in the equations for the vortex intensity and the enthalpy; 2) the total drop in enthalpy on the boundaries was introduced gradually, and in the first iteration the enthalpies at the input and on the walls were specified to be equal to the enthalpy at the electrode, and in subsequent iterations we carry out the calculations using the formula

$$H_{w,i}=(H_e-H_w)\exp(-i/i_1)+H_w,$$

where i is the number of the iteration, i_1 = 50-100; 3) the electrical conductivity at low temperatures was taken to be equal to a certain small quantity (its value was chosen in such

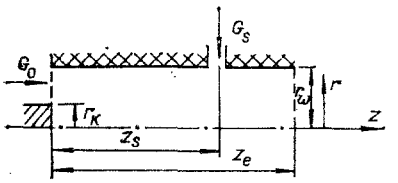

Fig. 1

a way that it has no effect on the solution obtained). In order to avoid spatial oscillations of the electric field in the low-temperature region, after calculating the fields using (1.2) we averaged them using the condition E = const in the nonconducting region.

2. As an example we will consider an electric arc burning in a sectioned channel of a plasmatron ($d_w = 10^{-2}$ m and $z_e = 0.11$ m). We will use argon at atmospheric pressure as the working gas. Keen blowing at a flow rate G_s through a section situated at a distance $z_s = 0.77 \cdot 10^{-1}$ m is employed. The calculations were carried out for the following parameters: $G_0 = 0.17 \cdot 10^{-3}$ kg/sec, $G_s = 0$, $0.92 \cdot 10^{-3}$, and $2.41 \cdot 10^{-3}$ kg/sec, I = 214 A, the gas temperature at the input and on the walls is 300°K, and on the electrode is $1.4 \cdot 10^4$ °K. For the calculations we used a nonuniform mesh (21 × 31) in the (z, r) plane.

In Fig. 2a we show the calculated temperature profiles (the continuous curves) and the experimental temperature profiles [2] in the blowing cross section for $G_s = 0$, and in Fig. 2b for $G_s = 2.41 \cdot 10^{-3}$ kg/sec. The difference in the behavior of the curves when there is sharp blowing is obviously due to the impossibility of correctly simulating the keen-blowing conditions. We used a specially profiled nozzle in the experiment for this purpose, and in the calculations the blowing velocity was assumed to be constant over the whole width of the slot ($5 \cdot 10^{-3}$ m). The presence of an intense radial flow of cold gas leads to contraction of the arc and to an increase in the axial temperature. In Fig. 3 the broken curves represent the conventional radius of the arc, found from the condition $T(r_d) = T_* = 7000$°K (when $T < T_*$ $\sigma \approx 0$). Note that contraction of the arc is also observed below with respect to the flow from the blowing section. In the blowing section a maximum of the electric field is observed, and when $z > z_s$ the electric field does not fall to its initial value. In Fig. 3 the points represent experimental values of the electric field obtained by differentiating the dependence of the section potential on the z coordinate for $G_s = 2.62 \cdot 10^{-3}$ kg/sec. In Fig. 4 we show the energy losses per unit length of the channel wall: the losses due to thermal conductivity

$$Q_T = -2\pi r_w \frac{\lambda}{c_p} \frac{\partial H}{\partial r}\Big|_{r=r_w}$$

and the overall losses

$$Q_s = Q_T + 2\pi \int_0^{r_w} F_R r\, dr.$$

Under these conditions the main mechanism of energy transfer is radiation. Keen blowing, which produces a gas curtain on the wall, when $z > z_s$ practically eliminates the flow of heat on the wall due to thermal conduction. In Fig. 4 the points 1 indicate the experimental values for $G_s = 0.92 \cdot 10^{-3}$ kg/sec, and the points 2 for $G_s = 0.89 \cdot 10^{-3}$ kg/sec. The lower calculated values of the loss are obviously due to ignoring the radiant component of the heat conduction at temperatures of the order of 10^4°K, which may play an important role. This

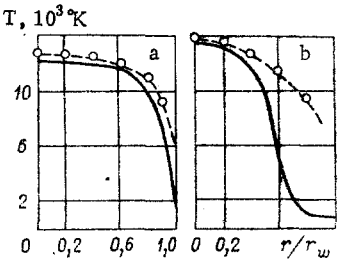

Fig. 2

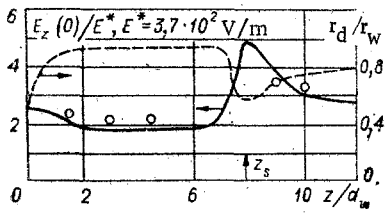

Fig. 3

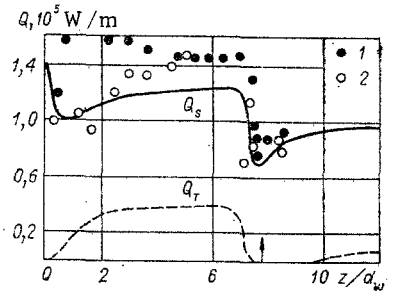

Fig. 4

leads to an increase in the thermal efficiency of the plasmatron (see Table 1), defined in the form

$$\eta_T = (IV - \Sigma Q)/IV,$$

where V is the burning voltage and ΣQ are the overall energy losses due to thermal conduction and radiation. In Fig. 5 we show profiles of the velocity U_Z for $G_S = 2.41\cdot10^{-3}$ kg/sec, and $z/d_W = 0.5$, 6, 7, 7.7, and 12 (curves 1-4, respectively). In Fig. 6 we show current lines (a), isotherms (b), and electric-current lines (c) for $G_S = 2.41\cdot10^{-3}$ kg/sec. In Fig. 7 we show electric-current lines for different positions of the anode.

The theoretical and experimental integral characteristics of the electric arc are compared in Table 1. Here the mean-mass enthalpy at the output of the plasmatron

$$\overline{H} = \int_0^{r_w} \rho u_z H r dr \left(\int_0^{r_w} \rho u_z r dr \right)^{-1};$$

and the integral Joule heat

$$Q_0 = 2\pi \int_0^{r_w} \int_0^{z_e} \sigma \left[E_z^2 + E_r^2 \right] r dr dz;$$

Q_T and Q_R are the integral losses due to thermal conduction and radiation, respectively, and Q_H is the loss due to convective transfer.

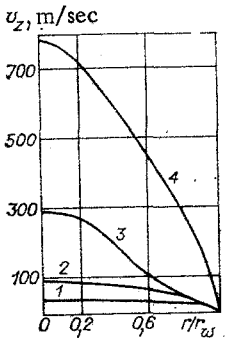

Fig. 5

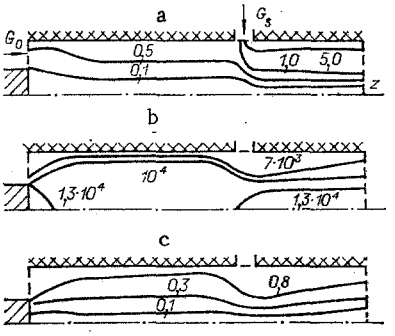

Fig. 6

TABLE 1

	Theor.	Theor.	Exper.		Theor.	Theor.	Exper.
G_s, 10^{-3} kg/sec	2,41	0,92	0,92	Q_0, kW	22,7	20,4	—
I V, kW	23,4	20,6	24,6	Q_T, kW	2,31	2,46	—
η_T, %	44,5	38	31,3	Q_R, kW	10,7	10,2	—
$\overline{H}$, 10^6 J/kg	3,9	6,75	7,08	Q_H, kW	10,1	7,23	—
V, V	109	96	115				

Fig. 7

The proposed method of calculation and the results obtained confirm the efficiency of the method of complete elliptic equations for determining local and integral characteristics of the electric arc. The distributions shown in Figs. 2-6 confirm the effectiveness of keen blowing and the unreliability of model estimates used to determine the plasma parameters in the case of keen blowing. Only by using calculations similar to those carried out in the present paper can one obtain suitable practical design relations. In addition, the proposed method of calculating the velocity profile and other plasma parameters can be used to investigate the transfer properties of a plasma, viz., the viscosity, the thermal conductivity, etc.

LITERATURE CITED

1. M. F. Zhukov, A. S. An'shakov, I. M. Zasypkin, et al., Electric Arc Generators with Interelectrode Mountings [in Russian], Nauka, Novosibirsk (1981).
2. Makhan and Kremers "An electric arc heater with arc stabilization by the channel walls and local gasdynamic compression of the discharge," Teor. Os. Inzh. Raschetov, No. 4 (1972).
3. Yu. V. Kurochkin and A. V. Pustogarov, "Investigation of a plasmatron in which the working solid is applied through a porous interelectrode mounting," in: Experimental Investigations of Plasmatrons [in Russian], Nauka, Novosibirsk (1977).
4. V. V. Berbasov and B. A. Uryukov, "A laminar electric arc in a channel with porous cooling of the walls," in: The Theory of the Electric Arc Under Conditions of Forced Heat Exchange [in Russian], Nauka, Novosibirsk (1977).
5. A. D. Gosmen, V. N. Pan, A. K. Ranchel, et al., Numerical Methods of Investigating the Flow of a Viscous Liquid [Russian translation], Mir, Moscow (1972).
6. A. N. Prokof'ev and G. B. Sinyarev, "Numerical investigation of an electric arc blown by a flow of gas," in: Proc. Seventh All-Union Conference on Low-Temperature Plasma Generators, Alma-Ata (1977).
7. A. S. Korneev, I. P. Nazarenko, and I. G. Panevin, "Numerical calculation of the characteristics of a channel arc blown by a concomitant flow of gas with twisting," in: Proc. Eighth All-Union Conference on Low-Temperature Plasma Generators [in Russian], Novosibirsk (1980).
8. A. B. Karabut, Yu. V. Kurochkin, and A. N. Prokof'ev, "Numerical investigation of an electric arc discharge in a permeable channel with intense blowing of a plasma-forming gas," Teplofiz. Vys. Temp., 19, No. 3 (1981).
9. J. E. Anderson, Transfer Phenomena in a Thermal Plasma [Russian translation], Énergiya, Moscow (1972).
10. P. Rouch, Computational Hydrodynamics [Russian translation], Mir, Moscow (1980).